Cryptotanshinone, a novel PDK 4 inhibitor, suppresses bladder cancer cell invasiveness via the mTOR/β-catenin/N-cadherin axis

CHUL JANG KIM[1,5], TOKIO TERADO[2], YUKIHIRO TAMBE[3], KEN-ICHI MUKAISHO[4], SUSUMU KAGEYAMA[5], AKIHIRO KAWAUCHI[5] and HIROKAZU INOUE[3]

[1]Department of Urology, Kohka Public Hospital, Minakuchi-cho, Kohka, Shiga 528-0074; [2]Department of Stem Cell Biology and Regenerative Medicine, [3]Division of Microbiology and Infectious Diseases, [4]Division of Human Pathology and [5]Department of Urology, Shiga University of Medical Science, Setatsukinowa-cho, Otsu, Shiga 520-2192, Japan

Received December 24, 2020; Accepted April 19, 2021

DOI: 10.3892/ijo.2021.5220

Abstract. The phosphorylation of pyruvate dehydrogenase (PDH) by pyruvate dehydrogenase kinase (PDK) 4 inhibits its ability to induce a glycolytic shift. PDK4 expression is upregulated in various types of human cancer. Because PDK4 regulation is critical for metabolic changes in cancer cells, it is an attractive target for cancer therapy given its ability to shift glucose metabolism. It was previously shown that a novel PDK4 inhibitor, cryptotanshinone (CPT), suppressed the three-dimensional (3D)-spheroid formation of pancreatic and colorectal cancer cells. In the present study, the effects of CPT on the invasiveness of bladder cancer cells were investigated. CPT significantly suppressed the invasiveness and 3D-spheroid formation of T24 and J82 bladder cancer cells. CPT also suppressed the phosphorylation of PDH and β-catenin, as well as the expression of N-cadherin, which are all critical for inducing epithelial-mesenchymal transition (EMT). The knockdown of β-catenin or PDK4 using specific small interfering RNAs suppressed N-cadherin expression and invasiveness in T24 cells. An mTOR inhibitor also suppressed the phosphorylation of β-catenin and N-cadherin expression. Furthermore, CPT injection significantly suppressed pancreatic tumor growth and peritoneal dissemination of highly metastatic SUIT-2 pancreatic cancer cells in a mouse orthotopic pancreatic cancer model, without evident toxicity. Moreover, immunohistochemistry analyses demonstrated decreased β-catenin expression in CPT-treated pancreatic tumors compared with control tumors. Taken together, these results indicate that CPT reduced the invasiveness and metastasis of bladder cancer cells by suppressing EMT via the mTOR/β-catenin/N-cadherin pathway.

Correspondence to: Dr Hirokazu Inoue, Division of Microbiology and Infectious Diseases, Shiga University of Medical Science, Setatsukinowa-cho, Otsu, Shiga 520-2192, Japan
E-mail: hirokazu@belle.shiga-med.ac.jp

Abbreviations: ATP, adenosine triphosphate; CPT, cryptotanshinone; DMSO, dimethyl sulfoxide; DMEM, Dulbecco's modified Eagle's medium; DCA, dichloroacetate; EMT, epithelial-mesenchymal transition; MIBC, muscle invasive bladder cancer; PDH, pyruvate dehydrogenase; PDK, pyruvate dehydrogenase kinase; poly-HEMA, poly-(2-hydroxyethyl methacrylate); siRNA, small interfering RNA; 3D, three-dimensional

Key words: PDK4 inhibitor, cryptotanshinone, bladder neoplasm, β-catenin, invasiveness

Introduction

Under aerobic conditions, the majority of proliferating cancer cells preferentially metabolize glucose via glycolysis, which is a primary metabolic hallmark of cancer cells (1-3). Pyruvate dehydrogenase kinases (PDKs) are key molecules in the mitochondria, which via decarboxylation, regulate the oxidative metabolism of pyruvate into acetyl-CoA. The physiological role of the PDK family is to phosphorylate the pyruvate dehydrogenase (PDH) complex (4). The inhibition of PDKs can restimulate the mitochondria metabolism of pyruvate in cancer cells (5), which subsequently inhibits tumor growth (6). Studies have revealed that the expression of PDK4, one of four PDK isoforms (PDK1-4), is frequently upregulated in various cancer types; thus, its regulation is critical for metabolic changes in cancer cells (7,8). Trinidad *et al* (9) reported that PDK4-knockdown using specific small interfering (si)RNAs suppressed lung and colorectal cancer cell proliferation, which suggests that PDK4 is an attractive target for cancer therapy. Despite reports demonstrating the therapeutic inhibition of PDK activity by dichloroacetate (DCA) (10-12), the half maximal inhibitory concentration necessary for PDK4 inhibition is in the range of 57.8-500 μM (7,13), and DCA exhibited reversible peripheral neuropathy in a number of clinical trials (10,14). Previous studies have attempted to identify novel compounds that can suppress PDK4 activity at sub-micromolar concentrations (13,14). Our previous study demonstrated that cryptotanshinone (CPT), which is obtained from the traditional Chinese herb *Salvia miltiorrhiza* Bunge (*danshen)*, effectively inhibited PDK4 activity at low concentrations (micromolar-order) to suppress malignant phenotypes, including three-dimensional (3D)-spheroid formation, anchorage-independent growth,

cellular proliferation and *in vivo* tumor growth of human pancreatic and colorectal cancer (15).

Invasiveness and metastasis are key defining characteristics of cancer cell malignancy, and metastasis is a major cause of cancer-associated death (16,17). Although invasiveness and metastasis are considered critical targets in the development of new therapeutic strategies, effective reagents that target these processes have yet to be identified. Previously, changes in energy metabolism have been shown to be closely associated with the invasive and metastatic abilities of cancer cells (18,19). Changes in cancer cell metabolism increase acid production in the cancer cells involved (20), which leads to normal cell death (21), extracellular matrix degradation by proteolytic enzymes (22), and enhanced migration and invasion capacity. Therefore, targeting cancer cell metabolism may provide a novel approach for inhibiting cancer cell invasiveness and metastasis, and result in more favorable treatment outcomes.

Bladder cancer is the 10th most common cancer type worldwide, with ~550,000 new cases diagnosed in 2018 (23). Bladder cancer is a complex disease associated with high morbidity and mortality rates. The treatment outcomes of radical cystectomy for muscle invasive bladder cancer (MIBC) combined with chemotherapy are insufficient (24), and the five-year survival rate is only ~5% in patients with metastatic bladder cancers (25). As there have been no significant improvements in the treatment outcome over the last three decades (26), new treatment strategies for MIBC and metastatic bladder cancers are necessary. PDK4 expression has been shown to be markedly higher in high-grade than in low-grade bladder cancers without the overexpression of PDK1, 2 or 3 (27). Therefore, the aim of the present study was to identify novel compounds to treat intractable bladder cancer by investigating the effects of CPT on the invasive and metastatic capacity of human bladder cancer cells.

Materials and methods

Cell culture. The human bladder cancer cell lines (T24 and J82) were cultured with RPMI-1640 (Nacalai Tesque, Inc.) supplemented with 10% fetal calf serum (FCS; Sigma-Aldrich; Merck KGaA), penicillin (100 U/ml; Meiji Seika Pharma, Co., Ltd.) and streptomycin (100 μg/ml; Meiji Seika Pharma, Co., Ltd.), at 37˚C (5% CO_2) in a humidified atmosphere. The SUIT-2 human pancreatic cancer cell line was cultured in Dulbecco's modified Eagle's medium (DMEM, Nacalai Tesque, Inc.). Additionally, a nonadherent culture was created by coating the culture dishes with poly-(2-hydroxyethyl methacrylate) reagent (poly-HEMA; Sigma-Aldrich; Merck KGaA). T24 cells were purchased from the American Type Culture Collection in 2000, and maintained in our laboratory. J82 and SUIT-2 cells were purchased from the American Type Culture Collection in 2019 and the Japanese Collection of Research Bioresources Cell Bank (Osaka, Japan) in 2018, respectively. The T24 cell line was authenticated by short tandem repeat analysis in 2018, as previously described (28).

Reagents. CPT was purchased from Cosmo Bio Co., Ltd., and was dissolved in dimethyl sulfoxide (DMSO) to prepare 10-mM stock solutions for the *in vitro* experiments. IL-6-hydroxymethyl-chiro-inositol2(R)-2-O-methyl-3-O-octadecylcarbonate (Akt inhibitor, Calbiochem; Merck KGaA), temsirolimus (Tokyo Chemical Industry Co., Ltd.) and PD98059 (Cell Signaling Technology, Inc.) were dissolved in DMSO to prepare the 20-mM stock solutions for the *in vitro* experiments. The same volume of DMSO was added to the control samples in all experiments.

3D-spheroid formation assay. The 3D-spheroid formation assay was performed using 96-well V-bottom plates (PrimeSurface®; Sumitomo Bakelite Co., Ltd.) as previously described (28). Briefly, $1x10^3$ cells were seeded in triplicate into each well in complete culture medium. After three days of incubation at 37˚C (5% CO_2) in a humidified atmosphere, images of spheroid formation were captured using phase contrast microscopy (magnification, x4; Olympus Corporation). To determine the number of viable cells in the 3D-spheroid, the ATP content was quantified using the luminescence-based CellTiter-Glo® 3D cell viability assay (Promega Corporation) according to the manufacturer's protocol. The Caspase-Glo® 3/7 assay (Promega Corporation) was used to measure caspase-3 and -7 activities according to the manufacturer's protocol.

In vitro invasion assay. The *in vitro* invasive potential of cancer cells was determined using a Matrigel™ Basement Membrane Matrix Invasion Chamber (chamber size, 6.4 mm; membrane surface area, 0.3 cm^2; pore size, 8 μm; BD Biosciences), according to the manufacturer's instructions (29). A total of 500 μl cell suspension ($2x10^4$ T24 and $4x10^4$ J82 cells/ml) was added to each chamber, and incubated for two or three days, respectively, at 37˚C in a humidified 5% CO_2 atmosphere. Culture medium without FCS was used in upper chambers, and 750 μl culture medium with 10% FCS was added to the lower chambers. Non-invasive cells were removed from the upper surface of the membrane using a cotton swab. The invasive cells on the underside of the membrane were harvested using Diff-Quik™ (Kokusai Shiyaku Co., Ltd.) and counted under a light microscope (magnification, x100). The duration of each Diff-Quik™ staining step was 3 min at room temperature. Each sample was then analyzed in triplicate.

Cell cycle analysis. Cell cycle distribution was evaluated using the Cycletest Plus DNA Reagent kit with a FACSCalibur flow cytometer system and ModFit 3.2 software (both Becton, Dickinson and Company). Briefly, the cells were collected after treatment with CPT (0, 10 and 20 μM at 37˚C for 24 h) and fixed in 70% ethanol at -20˚C for 18 h. The cells were washed twice with phosphate-buffered saline and then pelleted by centrifugation at 400 x g at room temperature for 5 min. The cell pellets were incubated with 250 μl solution A (trypsin in a spermine tetrahydrochloride detergent buffer) at room temperature for 10 min, 200 μl solution B (trypsin inhibitor and ribonuclease A in citrate stabilizing buffer with spermine tetrahydrochloride) at room temperature for 10 min, and then 200 μl solution C (propidium iodide and spermine tetrahydrochloride in citrate stabilizing buffer) in the dark at 4˚C for 10 min. The cells were then flow cytometrically.

Small interfering RNA (siRNA) transfection. For the siRNA experiment, cells were transfected with 50 nM Silencer® Select PDK4 siRNA (s10262; Thermo Fisher Scientific, Inc.) and β-catenin siRNA (sense; 5'-CAGGGGGUUGUG

GUUAAGCUCUU-3', antisense; 5'-AAGAGCUUAACC ACAACCCCCUG-3') (30) using Lipofectamine® RNAiMax (Invitrogen; Thermo Fisher Scientific, Inc.) for 24 h according to the manufacturer's protocol. A non-specific siRNA duplex (GeneDesign, Inc.) served as the control.

Western blotting. The 60-mm culture dishes were precoated with poly-HEMA at room temperature for 24 h. A total of $5x10^5$ cells were seeded into a poly-HEMA-coated dish, and cultured with CPT for 48 h (37˚C) under nonadherent culture conditions. Cell lysate preparation and western blotting were conducted as previously described (31). Amersham ECL western blotting detection kit (Cytiva) was used for visualization according to the manufacturer's protocol. The experiments were repeated at least three times. Mouse monoclonal antibodies for α-tubulin (1:1,000; DM1A, cat. no. T9026) were purchased from Sigma-Aldrich; Merck KGaA. Mouse monoclonal antibodies for E-cadherin (1:500; 36/E, cat. no. 610181) were purchased from BD Biosciences. Anti-PDH mouse monoclonal antibodies (1:500; cat. no. ab110330), anti-phospho-PDH rabbit polyclonal antibodies (1:500; S293; cat. no. ab92696), and anti-PDK4 rabbit polyclonal antibodies (1:500; cat. no. ab63157) were purchased from Abcam. Rabbit monoclonal antibodies for 4E-BP1 (1:500; 53H11, cat. no. #9644), phospho-4E-BP1 (1:500; S65, 174A9, cat. no. #9456), phospho-Akt (1:500; S473, D9E, cat. no. #4060), Erk1/2 (1:500; 137F5, cat. no. #4695), phospho-Erk1/2 (1:500; T202/Y204, 20G11, cat. no. #4376), MEK1/2 (1:500; 47E6, cat. no. #9126), phospho-MEK1/2 (1:500; S221, 166F8, cat. no. #2338), S6K (1:500; 49D7, cat. no. #2708), phospho-S6K (1:500; T421/S424, #9204), β-catenin (1:500; D10A8, #8480), phospho-β-catenin (1:500; S552, D8E11, cat. no. #5651), N-cadherin (1:500; D4R1H, cat. no. #13116), and caspase-3 (1:500; 8G10, cat. no. #9665); rabbit polyclonal antibodies for Akt (1:500; cat. no. #9272) and phospho-β-catenin (1:500; S33/37/T41, #9561); and mouse monoclonal antibodies for CD44 (1:1,000; 156-3C11, cat. no. #3570) and epithelial cell adhesion molecule (EpCAM) (1:500; VU1D9, cat. no. #2929) were purchased from Cell Signaling Technology, Inc. Rabbit polyclonal antibodies for lamin A/C (1:500; cat. no. #10298-1-AP) were purchased from ProteinTech Group, Inc. The horse radish peroxidase-conjugated anti-mouse IgG (1:10,000, cat. no. NA931, from sheep) and anti-rabbit IgG (1:10,000, cat. no. NA934, from donkey) secondary antibodies were purchased from Cytiva. Caspase-3 control cell extracts (cat. no. #9663) for the negative and positive controls for apoptosis analysis were purchased from Cell Signaling Technology, Inc.

Subcellular fractionation. Cytoplasmic and nuclear protein fractions were extracted using NE-PER® cytoplasmic and nuclear extraction regents (Pierce; Thermo Fisher Scientific, Inc.) according to the manufacturer's protocol. Western blot analysis was used to analyze the extracted protein samples. α-tubulin and lamin A/C were used as cytoplasmic and nuclear endogenous controls, respectively.

Laboratory animals. A total of 10 female, five-week-old *BALB/c-nu/nu* nude mice (5 control and 5 CPT-treated mice, weight 16-18 g) were purchased from CLEA Japan and housed in a specific pathogen-free room with controlled temperature (20-22˚C) and humidity (50-60%), and a preset light-dark cycle (12:12 h). All mice were allowed *ad libitum* access to food (CE-2; CLEA Japan, Inc.) and water. The use of animals in the experimental protocols was reviewed and approved by the Management Committee of the Research Center for Animal Life Science at Shiga University of Medical Science (Shiga, Japan).

Orthotopic pancreatic cancer model of nude mice. A total of 10 5-week-old mice were anesthetized by intraperitoneal injection of pentobarbital (50 mg/kg) and maintained by inhalation of 1% isoflurane. The abdominal cavity was opened using a 1.5-cm wide longitudinal laparotomy pointing slightly to the left. Then, $2x10^5$ SUIT-2 cells in 100 μl DMEM were injected into the tail of the pancreas with a 27-gauge needle. Both the operation and injection were performed by the same person (CJK and YT, respectively). The pancreas was placed back into the abdominal cavity, which was then closed using interrupted suturing with 4-0 Nylon, and penicillin G (200 U/20 g) was injected intramuscularly to prevent postoperative infection. After seven days, five mice were intraperitoneally administered 40 mg/kg of CPT (suspended in 8% DMSO and 2% Solutol) every two days for two weeks. The control mice were administered a vehicle (8% DMSO and 2% Solutol) every two days for two weeks. Finally, the mice were sacrificed by cervical dislocation one day after the last administration. The pancreas, heart, lungs, liver and kidneys were resected and fixed with 10% buffered formalin at 4˚C for 24 h. The intestine with the mesentery were also resected, and the tumor nodules of the mesentery were counted macroscopically. The volume of the largest tumor nodule in one mouse was calculated using the following formula: $3.14xAxB^2/6$, where A and B represent the long and short diameters, respectively. A and B were measured using the histological preparations of hematoxylin and eosin staining.

Histopathological analyses. Serial 3-μm sections of formalin-fixed (10%, 4˚C for 24 h), paraffin-embedded tissues were histologically evaluated by hematoxylin and eosin staining and light microscope. For the immunohistochemical analyses, dewaxed sections were assessed using β-catenin antibodies via the streptavidin-biotin-peroxidase method [Histofine® MAX-PO (MULTI); Nichirei Biosciences, Inc.], according to the manufacturer's instructions.

Statistical analyses. All quantitative data are presented as the mean ± standard deviation. One-way ANOVA following by Tukey's test for multiple comparisons, Wilcoxon's rank sum test, and Welch's t-test were used for the statistical analyses. All analyses were performed using the R statistical software package, version 2.6.2 (https://www.r-project.org/), and $P<0.05$ was considered to indicate a statistically significant difference.

Results

Effects of CPT on bladder cancer cell invasiveness in vitro. To assess the suppressive activity of CPT on the invasiveness of human bladder cancer, its effects on the 3D-spheroid formation and invasiveness of two human bladder cancer cell lines (T24 and J82) were investigated. The effect of CPT on

PDK4 activity was evaluated by monitoring the phosphorylation PDH, the target protein of PDK4. Under nonadherent culture conditions, 10-20 μM CPT effectively suppressed PDH phosphorylation at serine 293, a hallmark of PDH activity (32), in a dose-dependent manner (Fig. 1A). The expression levels of PDH and α-tubulin (the internal control protein) remained unaffected by CPT treatment, while PDK4 expression was suppressed by 20 μM CPT. The antioncogenic effect of CPT was assessed by evaluating T24 and J82 cell 3D-spheroid formation, a method is frequently used in cancer research to more closely mimic the tumor environment (33). 3D-spheroid formation was morphologically altered in these cell lines by CPT treatment (3-10 μM; Fig. S1). The edge of the spheroid became less distinct following CPT treatment. Moreover, CPT treatment (3-20 μM) significantly decreased the ATP concentration in these cell lines in a dose-dependent manner, which is closely associated with the number of viable cancer cells in the spheroids (Fig. 1B). Furthermore, the invasiveness of both cell lines was significantly suppressed by CPT treatment (Fig. 1C-D). The induction of apoptosis was also assessed by monitoring the cleavage of caspase-3. Caspase-3 activation (cleaved, lower band) was not detected in T24 and J82 cells (Fig. 1E). Furthermore, the Caspase-Glo® 3/7 assay was used to measure caspase-3 and -7 activities. The number of viable cells in 3D-spheroids was assessed using ATP activity in T24 and J82 cells. There were significantly fewer viable T24 and J82 cells following CPT treatment (Fig. S2A). Similarly, the caspase-3/7 activities decreased in these cells, and the caspase-3/7/ATP activity ratio was not increased following CPT treatment (Fig. S2B-C). This result was most likely due to the decrease in caspase-3/7 activities reflecting the decrease in the viable number of T24 and J82 spheroids after CPT treatment. Furthermore, flow cytometry was used to assess the pro-apoptotic effect of CPT. As shown in Figs. 1F and S3, CPT treatment increased the sub-G_1 fraction at a concentration of 20 μM in both cell lines. These results indicate that CPT suppressed invasiveness and 3D-spheroid formation in bladder cancer cells, and that apoptosis may play a partial role in these anti-oncogenic activities.

Alterations in invasion-related proteins following CPT treatment. To clarify the molecular mechanisms by which CPT suppresses cellular invasiveness, changes in the expression of proteins associated with epithelial-mesenchymal transition (EMT) were evaluated in T24 and J82 cells. Figs. 2A and S4 show that CPT treatment significantly decreased N-cadherin expression in a dose-dependent manner. However, E-cadherin expression was not detected in these cells. A CPT concentration of 10-20 μM also suppressed β-catenin phosphorylation at S552 in a dose-dependent manner. β-catenin phosphorylation at S552 induces β-catenin accumulation in the nucleus and increases its transcriptional activity (34). However, 10 μM CPT enhanced β-catenin phosphorylation at S33/S37/T41, which has been shown to promote its ubiquitylation and proteasomal degradation (35,36). In the present study, CPT treatment at 20 μM suppressed both total β-catenin expression and β-catenin phosphorylation at S33/S37/T41 (Figs. 2A and S4). This dual function of CPT for β-catenin phosphorylation is thought to be responsible for the suppression of cell invasiveness via β-catenin suppression. A subcellular fractionation assay was then performed to detect changes in the subcellular localization of β-catenin in T24 cells (Fig. 2B). CPT treatment significantly suppressed the phosphorylation of β-catenin at S552 and its accumulation in the nucleus. By contrast, the levels of β-catenin and phosphorylated β-catenin at S552 in the cytoplasm were weakly decreased by CPT, compared with the levels in the nucleus. The β-catenin signaling pathway has been reported to play a crucial role in the EMT process via the nuclear translocation of β-catenin (37). Therefore, these results indicate that CPT can effectively suppress the accumulation of β-catenin in the nucleus.

Since 3D-spheroid formation is considered to be a phenotype of cancer stem cells (15), and because these spheroids are associated with invasiveness (28), alterations in the expression of CD44 and EpCAM, which are stem cell markers of human bladder cancer, were investigated in T24 and J82 cells. Changes in cancer-related signaling pathway proteins, such as those of the MEK/Erk, Akt and mTOR cascades, were also investigated. As shown in Figs. 2A and S4, CPT suppressed the cancer stem cell phenotypes of these cells. Additionally, CPT suppressed MEK and Erk phosphorylation (Fig. 2C). Furthermore, CPT treatment decreased Akt phosphorylation at S473 and suppressed the phosphorylation of S6K (Fig. S4) and 4E-BP1, the target proteins of mTOR kinase (Fig. 2C). These results indicate that CPT suppressed the MEK/Erk, Akt and mTOR signaling pathways in these bladder cancer cell lines.

The role of β-catenin in the CPT-induced suppression of N-cadherin expression and cellular invasiveness. To confirm whether the alterations in EMT-associated protein levels, growth-associated signaling pathways, and cancer stemness markers induced by CPT were the result of inhibited PDK4 activity, PDK4 expression was knocked down in T24 cells, which effectively suppressed the expression of PDK4 and PDH phosphorylation (Fig. 3A). PDK4-knockdown significantly decreased ATP concentration and suppressed cellular invasiveness, as well as altering the morphology of the spheroid (Figs. 3B and C, and S5). As shown in Fig. 3D, it also suppressed the phosphorylation of β-catenin at S552, N-cadherin expression, the MEK/Erk, Akt and mTOR signaling pathways, and CD44 expression. However, PDK4-siRNA did not alter β-catenin phosphorylation at S33/S37/T41. Taken together, these results support the finding that the suppressive effects caused by CPT were the result of PDK4 inactivation.

To clarify the roles of N-cadherin and β-catenin in the CPT-induced suppression of invasiveness, β-catenin was knocked down in T24 cells. β-catenin-siRNA significantly decreased the ATP concentration and suppressed cellular invasiveness, 3D-spheroid formation, and β-catenin expression (Figs. 3B, C and E, and S5). Phosphorylation at S552 and N-cadherin expression were also suppressed (Fig. 3E). The MEK/Erk, Akt and mTOR signaling pathways, as well as CD44 expression, were not affected by the β-catenin-knockdown. These results demonstrate that the inactivation of β-catenin plays a crucial role in suppressing cellular invasiveness; moreover, N-cadherin acts downstream of β-catenin to suppress the invasiveness induced by CPT. To assess the roles of Erk, Akt and mTOR in the suppression of β-catenin and N-cadherin, T24 cells were treated with inhibitors of these kinases. As shown in Fig. 4, the inhibitors (40 μM) acted on their target

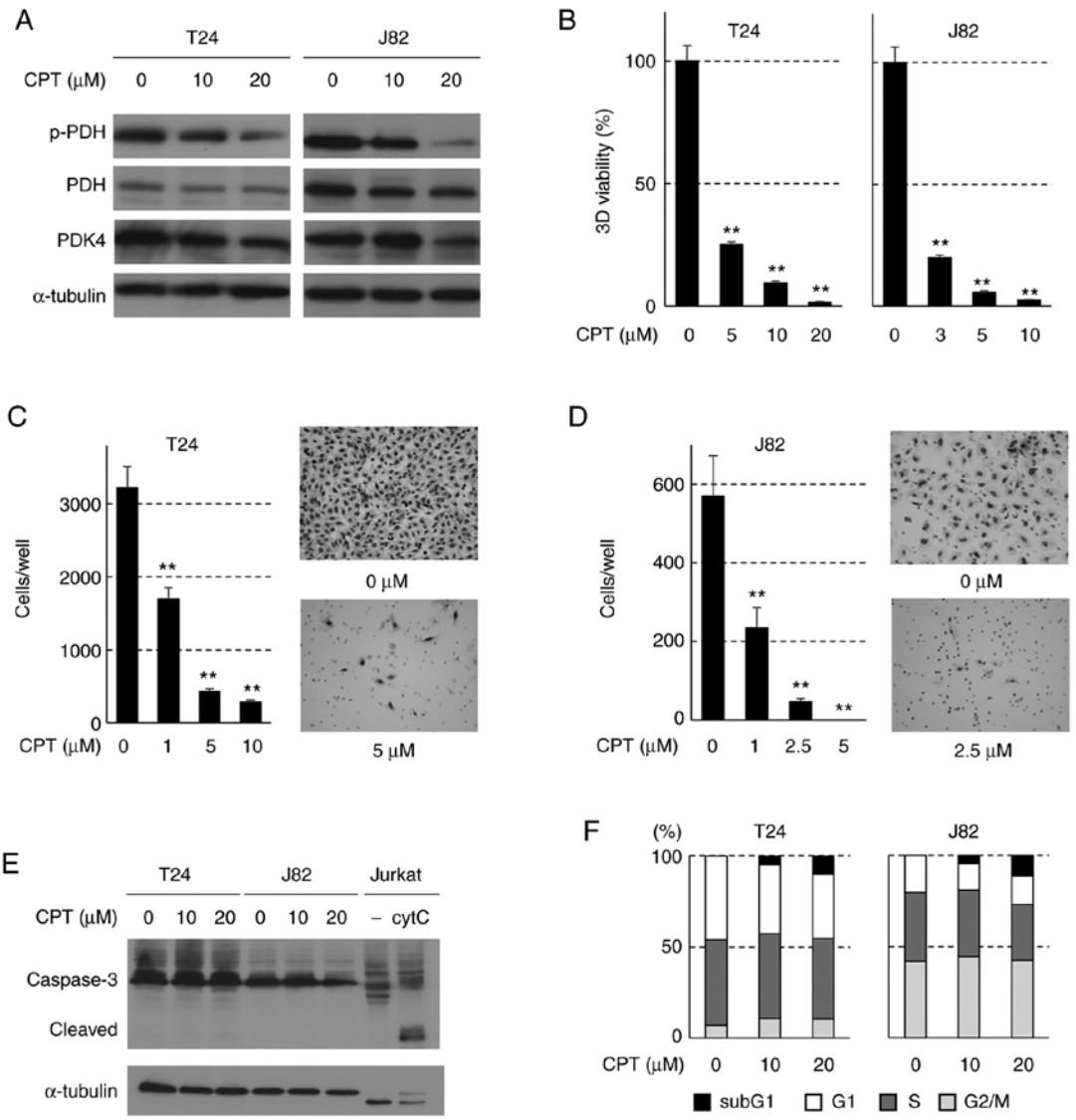

Figure 1. Effects of CPT on the invasiveness of human bladder cancer cells *in vitro*. (A) Western blot detection of PDH and PDK4 in T24 and J82 cells treated with CPT for 48 h. α-tubulin was used as the internal control. (B) Effects of CPT on the viability of spheroids formed from T24 and J82 cells. Bars indicate the mean ± SD. Adenosine triphosphate content was assessed using CellTiter-Glo® 3D assays. **P<0.001 compared with untreated cells using Tukey's test. Effects of CPT on the invasiveness of (C) T24 and (D) J82 cells. Each sample was assayed in triplicate, and the bars represent the mean ± SD. Images of T24 cells invading the Matrigel membrane. Images were captured at x100 magnification. **P<0.001 compared with untreated cells using Tukey's test. (E) Western blot analysis of caspase-3 cleavage in T24 and J82 cells treated with CPT. Untreated (-) or cytC-treated Jurkat cell extracts (caspase-3 control cell extracts, Cell Signaling Technology, Inc.) were used as negative or positive controls, respectively. α-tubulin was used as the internal control. (F) Apoptotic cytotoxicity of CPT in T24 and J82 cells. Stacked bars indicate the cell cycle profiles after treatment with CPT for 24 h; the sub-G1 fraction, presented as the black area on the top of each bar, indicates the proportion of the apoptotic cells. CPT, cryptotanshinone; PDH, pyruvate dehydrogenase; PDK4, pyruvate dehydrogenase kinase 4; p-, phosphorylated; cytC, cytochrome C.

kinases to suppress the mTOR targets, and the phosphorylation of S6K and 4EBP1 (Fig. 4A), Akt (Fig. 4B) and Erk (Fig. 4C). Although Akt and Erk inhibitors could not suppress β-catenin phosphorylation at S552 and N-cadherin expression, the mTOR inhibitor, temsirolimus, suppressed β-catenin phosphorylation at S552 and N-cadherin expression (Fig. 4D). These results indicate that the mTOR pathway acts upstream of β-catenin/N-cadherin in T24 cells. Additionally, Akt, mTOR, and Erk inhibitors did not suppress CD44 expression (Fig. 4D), indicating that the downregulation of CD44 by CPT occurs independently of these signaling pathways.

Antioncogenic effects of CPT in an in vivo orthotopic pancreatic cancer model of nude mice. To investigate the effects of CPT on *in vivo* metastasis, the aim was to establish a subcutaneous cancer cell xenograft model of lung metastasis via injection of J82 cells into the tail vein, and a liver metastasis model via injection into the spleens of nude mice. However, J82 metastatic tumors could not be detected in these experimental models. Therefore, an orthotopic pancreatic cancer model was created, which closely mimics pancreatic tumor formation using the highly metastatic pancreatic cancer cell line, SUIT-2 (38). The effects of CPT treatment in SUIT-2 cells were similar to those in bladder cancer cells; specifically, multiple oncogenic signaling pathways components were suppressed, including the phosphorylation of PDH and β-catenin at S552, and the expression of N-cadherin and CD44 (Fig. 5A). SUIT-2 cells were injected into the pancreases of nude mice, and

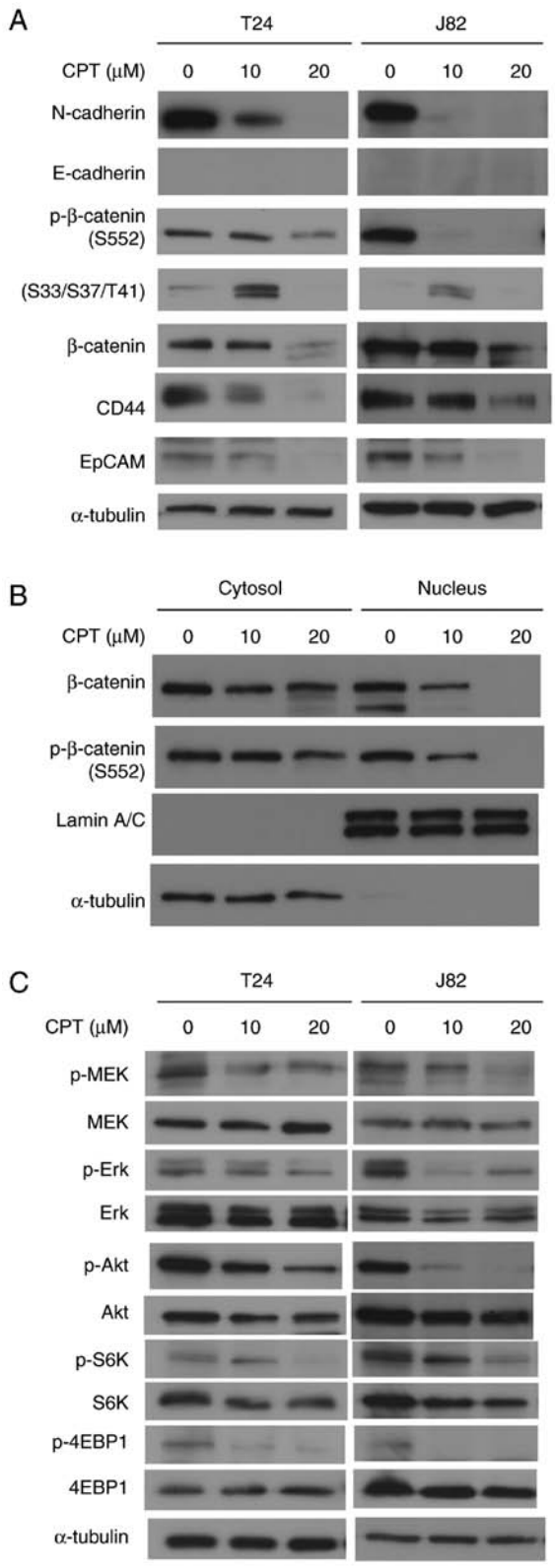

Figure 2. Alterations in cancer-related protein expression following CPT treatment. (A) Western blot analysis of proteins that regulate epithelial-mesenchymal transition and stemness in T24 and J82 cells treated with CPT for 48 h. α-tubulin was used as the internal control. (B) Subcellular localization of β-catenin and phosphorylated β-catenin (S552) in T24 cells treated with CPT for 48 h. Fractionated cytosolic and nuclear proteins were analyzed by western blotting using α-tubulin and lamin A/C antibodies, respectively. (C) Western blot analysis of MEK/Erk, Akt, and mTOR pathway proteins in the T24 and J82 cells treated with CPT for 48 h. α-tubulin was used as the internal control. CPT, cryptotanshinone; p-, phosphorylated; EpCAM, epithelial cell adhesion molecule; 4EBP1, eukaryotic translation initiation factor 4E-binding protein 1.

after one week, CPT was repeatedly administered (40 mg/kg, intraperitoneally) every two days for two weeks. At day 1 post-injection, SUIT-2 cells formed a pancreatic cancer-like tumor and disseminated nodules of the mesentery. Pancreatic tumor formation was moderately suppressed by CPT treatment in the pancreatic orthotopic cancer model (Fig. 5B-D). The volume of the largest tumor nodule in one mouse was 0.011±0.008 and 0.061±0.028 ml in CPT-treated and control groups, respectively. CPT treatment significantly decreased tumor growth in the pancreatic orthotopic cancer model (P=0.005). Furthermore, histopathological analyses revealed that tumor morphology in the CPT-treated mice was similar to that in the control mice. However, β-catenin was diffusely expressed in the cytoplasm of pancreatic cancer cells, while this was observed at the cytoplasmic membrane in normal pancreatic cells (Fig. 5E). β-catenin expression was markedly suppressed in the CPT-treated pancreatic tumors compared with the control tumors (Fig. 5F), and there were significantly fewer tumor nodules in the mesenterium after CPT treatment compared with the control tumors (Fig. 5G-I). Although histopathological examinations of the heart, lungs, liver and kidneys were also performed, no side effects from CPT treatment were observed under these experimental conditions. These results indicate that CPT suppressed *in vivo* tumor growth and peritoneal dissemination in an orthotopic pancreatic cancer model of nude mice.

Discussion

In the present study, CPT, a novel PDK4 inhibitor, was shown to suppress the invasiveness of bladder cancer cells *in vitro*. Furthermore, CPT inhibited *in vivo* tumor growth and peritoneal dissemination in an orthotopic pancreatic cancer model of nude mice. Although multiple molecular changes were observed in human bladder cancer cells following CPT treatment, including those of the β-catenin/N-cadherin, Erk, Akt and mTOR signaling pathways, as well as cancer stemness, siRNA-knockdown experiments highlighted the critical role of the β-catenin/N-cadherin axis in the suppression of cellular invasiveness downstream of PDK4 (Fig. 5J). Inhibitor experiments also indicated that CPT suppressed the β-catenin/N-cadherin axis via the mTOR pathway. As illustrated in Fig. 5J, CPT-associated inhibition of PDK4 leads to the suppression of mTOR. Downstream of mTOR, β-catenin was suppressed, causing the downregulation of N-cadherin expression, a master regulator of EMT in bladder cancer cells.

In the present study, CPT was revealed to exert a dual function in β-catenin phosphorylation. CPT (10 μM) enhanced β-catenin phosphorylation at S33/S37/T41 and suppressed phosphorylation at S552 in human bladder cancer cells. Phosphorylation of β-catenin at S33/S37/T41 has been shown to promote its ubiquitylation and proteasomal degradation (35,36). The suppression of β-catenin phosphorylation at S33/S37/T41 induced its cytoplasmic accumulation, and some of the free β-catenin translocated to the nucleus, resulting in deregulated cell cycle progression (35,36). Conversely, β-catenin phosphorylation at S552 is known to promote its transcriptional activity and cancer cell invasiveness (39). Therefore, CPT is considered to suppress the invasion of bladder cancer

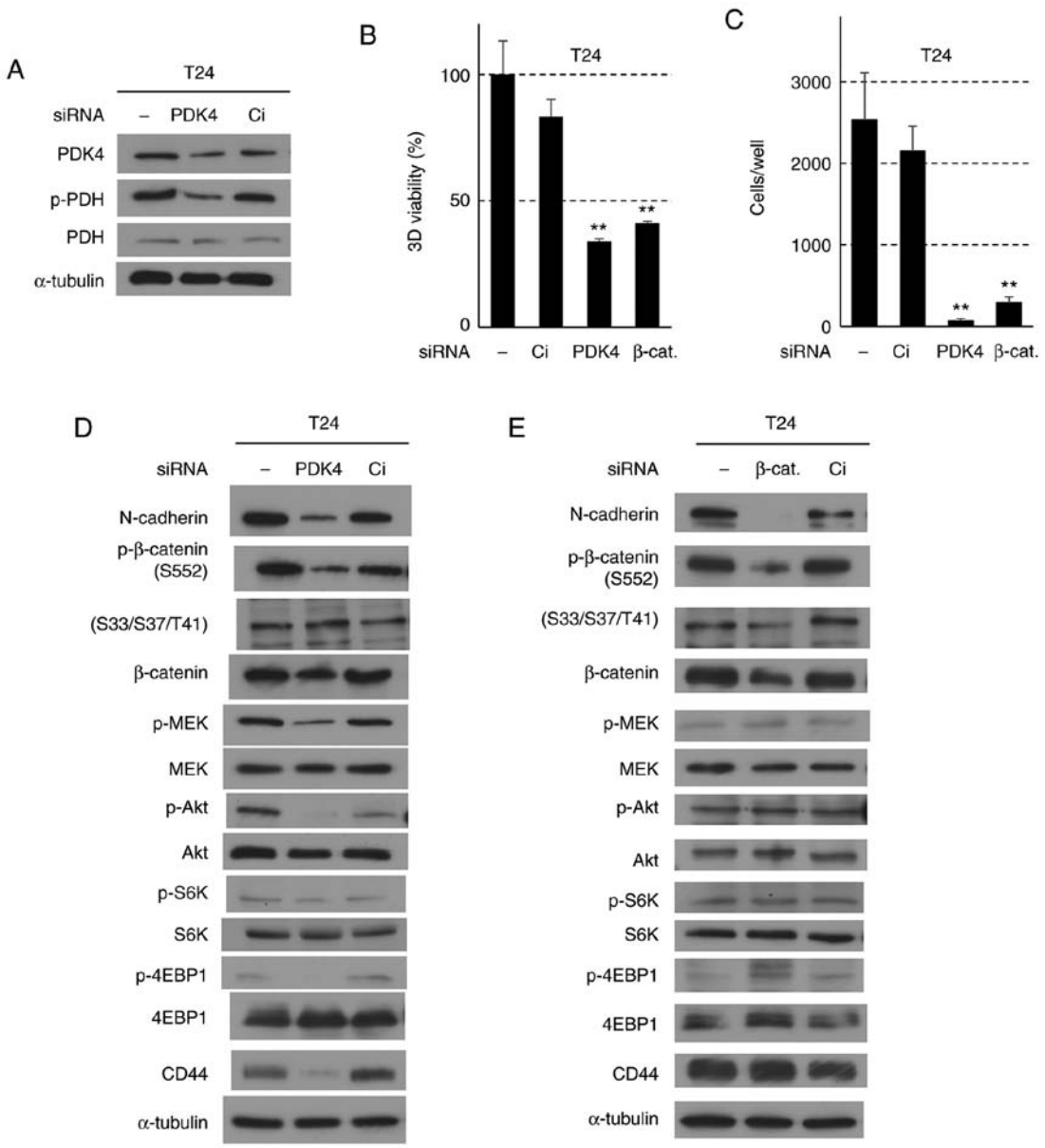

Figure 3. Effects of PDK4 and β-catenin siRNA-knockdown in T24 cells. Cells were treated with siRNA for 24 h, followed by nonadherent culture for 48 h, or 3D-spheroid formation for 72 h. (A) Western blot analysis for PDK4 and PDH proteins in T24 cells treated with Ci (siRNA control) and PDK4 siRNAs. α-tubulin was used as the internal control. (B) Effects of PDK4- and β-catenin-knockdown on the viability in T24 cells. Bars indicate the mean ± SD. Adenosine triphosphate content was assessed using the CellTiter-Glo® 3D assay. **P<0.001 compared with Ci control using Tukey's test. (C) Effects of siRNA for PDK4 and β-catenin on the invasiveness in T24 cells. Each sample was assayed in triplicate, and the bars represent the mean ± SD. **P<0.001 using Turkey's test compared with Ci control cells. (D and E) Western blot analysis for epithelial-mesenchymal transition, MEK, Akt, and mTOR pathway proteins in T24 cells treated with Ci, PDK4 and β-catenin siRNAs, respectively. α-tubulin was used as the internal control. CPT, cryptotanshinone; PDH, pyruvate dehydrogenase; PDK4, pyruvate dehydrogenase kinase 4; p-, phosphorylated; 3D, three-dimensional; Ci, siRNA control; 4EBP1, eukaryotic translation initiation factor 4E-binding protein 1.

cells by both promoting the ubiquitylation and degradation of β-catenin, as well as suppressing its transcriptional activity. In the present study, 20 μM CPT markedly suppressed β-catenin phosphorylation at S33/S37/T41 in bladder cancer cells, which appeared to be attributed to the decrease in total β-catenin expression due to its ubiquitylation and degradation. The enhanced nuclear accumulation of β-catenin has been observed in bladder cancer tissues, resulting in enhanced transcription of genes such as Snail and Twist (40). In the present study, β-catenin nuclear localization was decreased by CPT treatment in bladder cancer cells, which suggests that the alteration in β-catenin function is closely associated with CPT-induced suppression of tumor growth and cellular invasiveness.

CPT also suppressed the expression of cancer stem cell markers, CD44 and EpCAM, in bladder cancer cells, reflecting the inhibitory effect of CPT on cancer stem cell proliferation. In fact, CPT inhibited the representative phenotype of cancer stem cells and 3D-spheroid formation in bladder cancer cells. Furthermore, CPT significantly suppressed *in vivo* tumor growth and peritoneal dissemination in an orthotopic mouse model of SUIT-2 pancreatic cancer. CD44 is a cancer stem cell marker and a major surface receptor for hyaluronate, that has been shown to play a role in intracellular adhesion, cell-matrix adhesion, migration and tumor cell invasiveness and metastasis (41-43). Van Grevenstein *et al* (44) suggested that interference with CD44 may decrease the incidence of

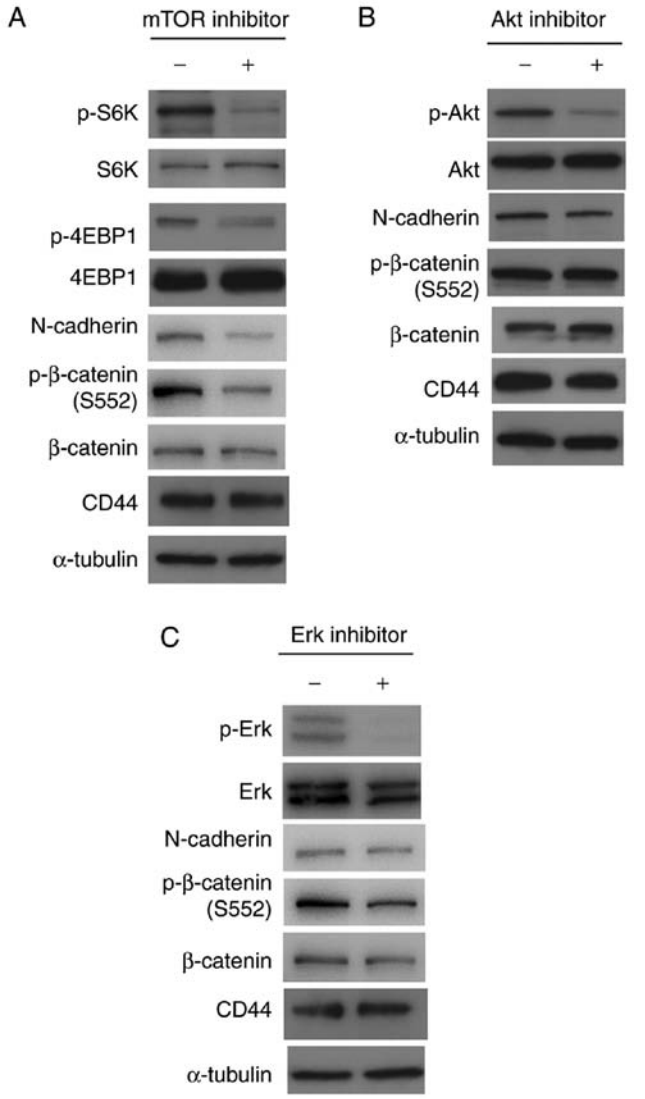

Figure 4. Effects of mTOR, Akt and Erk inhibitors in T24 cells. Western blot analysis following treatment with (A) the mTOR inhibitor, temsirolimus, (B) the Akt inhibitor [1L-6-hydroxymethyl-chiro-inositol 2-((R)-2-O-methyl-3-O-octadecylcarbonate)], and (C) the Erk inhibitor PD98059. (C) T24 cells were treated with each reagent at 40 μM for 48 h. α-tubulin was used as the internal control. 4EBP1, eukaryotic translation initiation factor 4E-binding protein 1.

peritoneal tumor recurrence after curative resection of pancreatic cancer. In bladder cancer, CD44, Oct4 and EpCAM have been shown to be highly expressed in, and associated with the progression of, bladder cancer (45,46). The present study also investigated the expression of Oct4 and retinal dehydrogenase 1. However, the expression of these proteins was low and not affected by CPT treatment in T24 and J82 cells (data not shown).

The mTOR signaling pathway has been reported to be a master regulator for the maintenance of cancer cell stemness (45,47,48). Previous research has demonstrated that cancer stem cells undergo metabolic alterations, including high glycolytic activity and low mitochondrial respiration (49). The results of the present study also suggest that the metabolic alterations caused by inhibiting PDK4 activity can suppress the stemness of bladder and pancreatic cancer cells. PDK4-knockdonwn analysis indicated that the inactivation of PDK4 contributed to decreased CD44 expression, although its suppression was independent of that of the mTOR/β-catenin/N-cadherin axis. N-cadherin has been shown to play a central role in the induction of EMT, which primarily contributes to the invasion and metastasis of malignant cancers (50). The dual suppression of CPT-induced EMT and cancer cell stemness via PDK4 inactivation may present a novel therapeutic approach for intractable malignant cancers.

The results of the present study also revealed that mTOR was a critical downstream target molecule of PDK4 for suppressing cellular invasiveness by CPT via β-catenin and N-cadherin. The mTOR (mTORC1) pathway is a central signaling pathway that controls metabolic processes (51,52). Studies using specific inhibitors have elucidated the role of mTOR in the control of cell proliferation and metabolism (53). The Wnt/β-catenin and Akt/mTOR pathways have been shown to be critically involved in colorectal cancer development (54) and are primarily regulated by feedback mechanisms. They are connected at multiple levels involving common upstream and downstream effectors. In the present study, mTOR acted upstream of β-catenin to suppress EMT and invasiveness following CPT administration. mTOR orchestrates metabolic reprogramming by regulating nutrient uptake and flux. Although various clinical trials have used rapamycin and its analogs, their therapeutic effects are limited by modest antitumor activity and increased toxicity. The results of the present study demonstrated that CPT was able to suppress the mTOR pathway, as well as other signaling cascades, at low concentrations. CPT also suppressed metastasis and tumor growth in an *in vivo* mouse orthotopic model without causing severe side effects. We also hypothesize that CPT and conventional mTOR inhibitors may synergistically suppress tumor growth, invasion and metastasis at low concentrations by altering cellular metabolism; however, the detailed mechanism by which PDK4 inactivation suppresses mTOR activity requires further investigation. Although our previous study investigated the inhibitory effect of CPT on PDK4 by *in vitro*, whether CPT can directly bind to and inhibit PDK4 *in vivo* remains to be elucidated.

Our previous study reported that CPT significantly inhibited the 3D-spheroid formation of pancreatic cancer cells at micromolar-order concentrations, without inducing apoptosis (15). In the current study, the induction of apoptosis was detected at low levels in T24 and J82 bladder cancer cells. Liu *et al* (55) reported that CPT promoted the apoptosis of bladder cancer cells in a dose-dependent manner. In their report, apoptosis was potently induced with 40-80 μM CPT, a higher concentration than that used in the present study (10-20 μM), suggesting that a difference in CPT concentration might contribute to the induction of apoptosis in bladder cancer cells. Furthermore, a low concentration of CPT was sufficient enough to suppress invasion and tumor growth, suggesting its potential as a clinical cancer therapy without considerable side effects. Cisplatin-based chemotherapy remains the standard first-line treatment for advanced bladder cancer (24), though patient outcomes remain insufficient. Thus, novel strategies for the treatment of advanced bladder cancer are required. The PDH-PDK axis has been considered a crucial therapeutic target in cancer (7,10,11) because PDK4 plays a pivotal role in the altered metabolism of malignant cancers (7,9). This

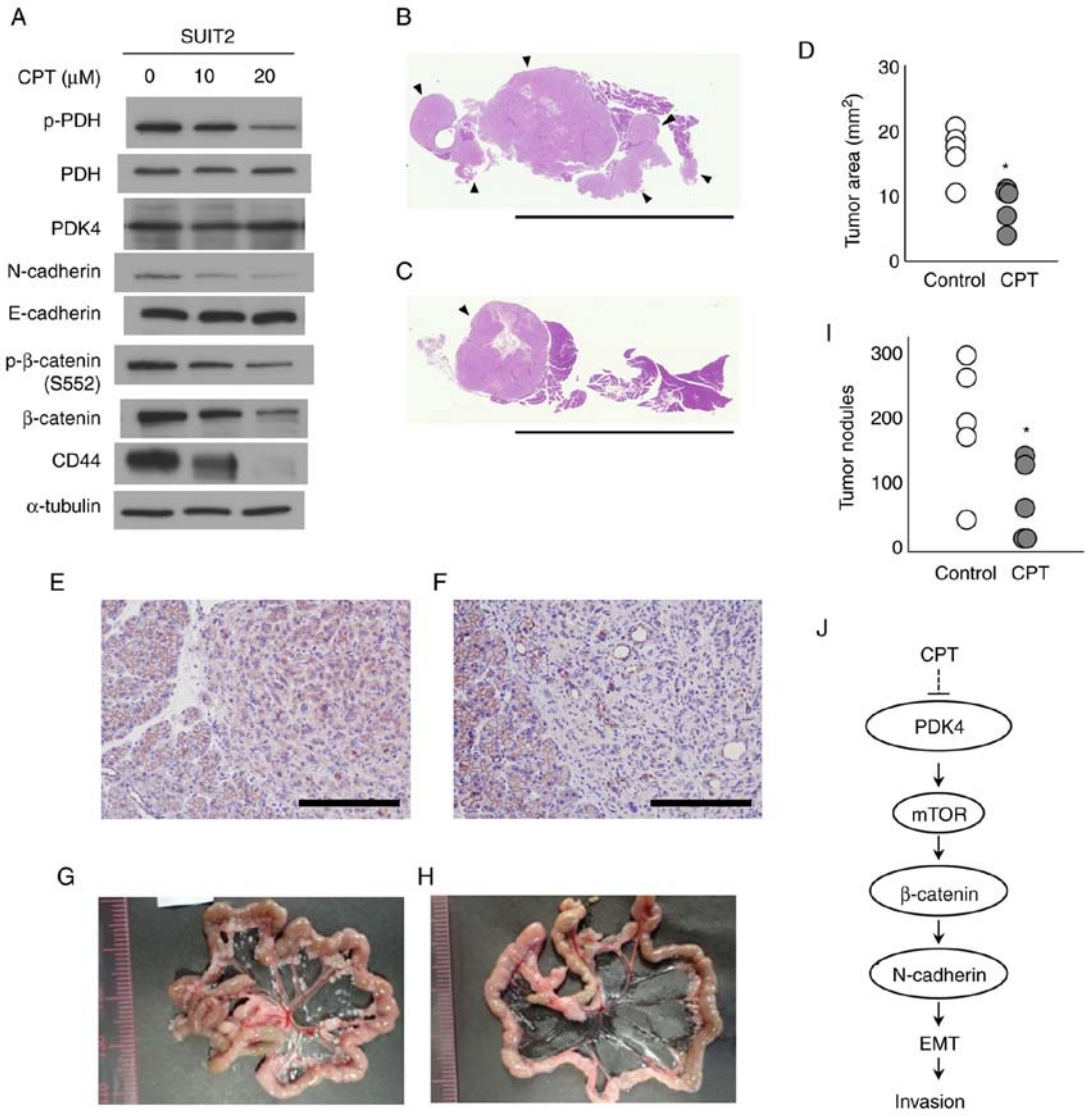

Figure 5. Effects of CPT in an *in vivo* orthotopic pancreatic cancer model of nude mice. (A) Western blot analysis for PDK4, PDH and proteins regulating EMT and cancer stemness in SUIT-2 cells, following treatment with CPT for 48 h. α-tubulin was used as the internal control. Low-magnification histological sections of the pancreas from the (B) control and (C) CPT-injected mice. Scale bar, 10 mm. Hematoxylin and eosin staining; arrows represent the tumor areas. (D) Tumor area size of the pancreas of SUIT-2 cells from the control and CPT-injected mice. *P<0.05 according to the Wilcoxon's rank sum test. Immunostaining for β-catenin of the pancreas from the (E) control and (F) CPT-injected mice. Scale bar, 200 μm; magnification, x200. Peritoneal metastatic nodules of SUIT-2 cells from the (G) control and (H) CPT-injected mice. (I) Number of peritoneal SUIT-2 cell metastatic nodules from the control and CPT-injected mice. *P<0.05 according to Wilcoxon's rank sum test. (J) Schematic illustration of the signaling pathway responsible for the suppressive effect of CPT on the invasiveness of bladder cancer cells. CPT, cryptotanshinone; PDH, pyruvate dehydrogenase; PDK4, pyruvate dehydrogenase kinase 4; p-, phosphorylated; EMT, epithelial-mesenchymal transition.

therapeutic strategy warrants small molecules that effectively inhibit PDK4 activity without exhibiting toxicity. However, the current findings on CPT will contribute to targeting or suppressing the invasion and metastasis of intractable malignant cancers.

Acknowledgements

The authors would like to thank Ms. Akiyo Ushio (Shiga University of Medical Science) for their technical assistance.

Funding

The present study was supported by the Japan Society for the Promotion of Scientific KAKENHI (Grants-in-Aid for Scientific Research from the Japan Society for the Promotion of Science), grant nos. 19K09687, 19K07480 and 19K07663.

Availability of data and materials

All data generated or analyzed during this study are included in this published article.

Authors' contributions

CJK and HI designed the study. CJK, TT, YT and HI performed and analyzed the experiments. KIM designed and performed the immunohistochemical analyses. SK and AK were involved in conceiving the project and provided several important suggestions to the research plan. CJK, TT, YT and HI wrote

the paper. CJK, TT and HI confirmed the authenticity of all the raw data. All authors read and approved the final manuscript.

Ethics approval and consult to participate

All animal experiments were performed in accordance with the care and use guidelines of Shiga University of Medical Science and approved by the Management Committee of the Research Center for Animal Life Science at Shiga University of Medical Science.

Patient consent for publication

Not applicable.

Competing interests

The authors declare that they have no competing interests.

References

1. Hanahan D and Weinberg RA: Hallmarks of cancer: The next generation. Cell 144: 646-674, 2011.
2. Hsu PP and Sabatini DM: Cancer cell metabolism: Warburg and beyond. Cell 134: 703-707, 2008.
3. Vander Heiden MG, Cantley LC and Thompson CB: Understanding the Warburg effect: The metabolic requirements of cell proliferation. Science 324: 1029-1033, 2009.
4. Sugden MC and Holness MJ: Mechanisms underlying regulation of the expression and activities of the mammalian pyruvate dehydrogenase kinases. Arch Physiol Biochem 112: 139-149, 2006.
5. Kinnaird A, Dromparis P, Saleme B, Gurtu V, Watson K, Paulin R, Zervopoulos S, Stenson T, Sutendra G, Pink DB, *et al*: Metabolic modulation of clear-cell renal cell carcinoma with dichloroacetate, an inhibitor of pyruvate dehydrogenase kinase. Eur Urol 69: 734-744, 2016.
6. Bonnet S, Archer SL, Allalunis-Turner J, Haromy A, Beaulieu C, Thompson R, Lee CT, Lopaschuk GD, Puttagunta L, Bonnet S, *et al*: A mitochondria-K^+ channel axis is suppressed in cancer and its normalization promotes apoptosis and inhibits cancer growth. Cancer Cell 11: 37-51, 2007.
7. Saunier E, Benelli C and Bortoli S: The pyruvate dehydrogenase complex in cancer: An old metabolic gatekeeper regulated by new pathways and pharmacological agents. Int J Cancer 138: 809-817, 2016.
8. Leclerc D, Pham DN, Lévesque N, Truongcao M, Foulkes WD, Sapienza C and Rozen R: Oncogenic role of PDK4 in human colon cancer cells. Br J Cancer 116: 930-936, 2017.
9. Trinidad AG, Whalley N, Rowlinson R, Delpuech O, Dudley P, Rooney C and Critchlow SE: Pyruvate dehydrogenase kinase 4 exhibits a novel role in the activation of mutant KRAS, regulating cell growth in lung and colorectal tumour cells. Oncogene 36: 6164-6176, 2017.
10. Stacpoole PW: Therapeutic targeting of the pyruvate dehydrogenase complex/pyruvate dehydrogenase kinase (PDC/PDK) axis in cancer. J Natl Cancer Inst: 109, 2017 doi: 10.1093/jnci/djx071.
11. Sutendra G and Michelakis ED: Pyruvate dehydrogenase kinase as a novel therapeutic target in oncology. Front Oncol 3: 38, 2013.
12. Kankotia S and Stacpoole PW: Dichloroacetate and cancer: New home for an orphan drug? Biochim Biophys Acta 1846: 617-629, 2014.
13. Yamane K, Indalao IL, Chida J, Yamamoto Y, Hanawa M and Kido H: Diisopropylamine dichloroacetate, a novel pyruvate dehydrogenase kinase 4 inhibitor, as a potential therapeutic agent for metabolic disorders and multiorgan failure in severe influenza. PLoS One 9: e98032, 2014.
14. Chu QS, Sangha R, Spratlin J, Vos LJ, Mackey JR, McEwan AJ, Venner P and Michelakis ED: A phase I open-labeled, single-arm, dose-escalation, study of dichloroacetate (DCA) in patients with advanced solid tumors. Invest New Drugs 33: 603-610, 2015.
15. Tambe Y, Terado T, Kim CJ, Mukaisho K, Yoshida S, Sugihara H, Tanaka H, Chida J, Kido H, Yamaji K, *et al*: Antitumor activity of potent pyruvate dehydrogenase kinase 4 inhibitors from plants in pancreatic cancer. Mol Carcinog 58: 1726-1737, 2019.
16. Fares J, Fares MY, Khachfe HH, Salhab HA and Fares Y: Molecular principles of metastasis: A hallmark of cancer revisited. Signal Transduct Target Ther 5: 28, 2020.
17. Dillekås H, Rogers MS and Straume O: Are 90% of deaths from cancer caused by metastases? Cancer Med 8: 5574-5576, 2019.
18. Kamarajugadda S, Stemboroski L, Cai Q, Simpson NE, Nayak S, Tan M and Lu J: Glucose oxidation modulates anoikis and tumor metastasis. Mol Cell Biol 32: 1893-1907, 2012.
19. Han T, Kang D, Ji D, Wang X, Zhan W, Fu M, Xin HB and Wang JB: How does cancer cell metabolism affect tumor migration and invasion? Cell Adh Migr 7: 395-403, 2013.
20. Gatenby RA and Gawlinski ET: The glycolytic phenotype in carcinogenesis and tumor invasion: Insights through mathematical models. Cancer Res 63: 3847-3854, 2003.
21. Williams AC, Collard TJ and Paraskeva C: An acidic environment leads to p53 dependent induction of apoptosis in human adenoma and carcinoma cell lines: Implications for clonal selection during colorectal carcinogenesis. Oncogene 18: 3199-3204, 1999.
22. Lardner A: The effects of extracellular pH on immune function. J Leukoc Biol 69: 522-530, 2001.
23. GLOBCAN 2018: Cancer fact sheet: Bladder. http://gco.iarc.fr/today/data/factsheets/cancers/30-Bladder-fact-sheet.pdf. Accessed December 22, 2020.
24. von der Maase H, Sengelov L, Roberts JT, Ricci S, Dogliotti L, Oliver T, Moore MJ, Zimmermann A and Arning M: Long-term survival results of a randomized trial comparing gemcitabine plus cisplatin, with methotrexate, vinblastine, doxorubicin, plus cisplatin in patients with bladder cancer. J Clin Oncol 23: 4602-4608, 2005.
25. Wahafu W, Liu S, Xu W, Wang M, He Q, Song L, Wang M, Yang F, Hua L, Niu Y and Xing N: The long-term efficacy of one-shot neoadjuvant intra-arterial chemotherapy combined with radical cystectomy versus radical cystectomy alone for bladder cancer: A propensity-score matching study. BMC Urol 19: 117, 2019.
26. Goto T and Miyamoto H: Why has the prognosis for muscle-invasive bladder cancer not significantly improved after decades of therapeutic advancements? Expert Rev Anticancer Ther 20: 229-231, 2020.
27. Woolbright BL, Choudhary D, Mikhalyuk A, Trammel C, Shanmugam S, Abbott E, Pilbeam CC and Taylor JA III: The role of pyruvate dehydrogenase Kinase-4 (PDK4) in bladder cancer and chemoresistance. Mol Cancer Ther 17: 2004-2012, 2018.
28. Kim CJ, Terado T, Tambe Y, Mukaisho K, Sugihara H, Kawauchi A and Inoue H: Anti-oncogenic activities of cyclin D1b siRNA on human bladder cancer cells via induction of apoptosis and suppression of cancer cell stemness and invasiveness. Int J Oncol 52: 231-240, 2018.
29. Kim CJ, Nishi K, Isono T, Okuyama Y, Tambe Y, Okada Y and Inoue H: Cyclin D1b variant promotes cell invasiveness independent of binding to CDK4 in human bladder cancer cells. Mol Carcinog 48: 953-964, 2009.
30. Zhang Q, Miao S, Han X, Li C, Zhang M, Cui K, Xiong T, Chen Z, Wang C and Xu H: MicroRNA-3619-5p suppresses bladder carcinoma progression by directly targeting β-catenin and CDK2 and activating p21. Cell Death Dis 9: 960, 2018.
31. Tambe Y, Hasebe M, Kim CJ, Yamamoto A and Inoue H: The drs tumor suppressor regulates glucose metabolism via lactate dehydrogenase-B. Mol Carcinog 55: 52-63, 2016.
32. Zhang W, Zhang SL, Hu X and Tam KY: Targeting tumor metabolism for cancer treatment: Is pyruvate dehydrogenase kinases (PDKs) a viable anticancer target? Int J Biol Sci 11: 1390-1400, 2015.
33. Weiswald LB, Bellet D and Dangles-Marie V: Spherical cancer models in tumor biology. Neoplasia 17: 1-15, 2015.
34. Fang D, Hawke D, Zheng Y, Xia Y, Meisenhelder J, Nika H, Mills GB, Kobayashi R, Hunter T and Lu Z: Phosphorylation of beta-catenin by Akt promotes beta-catenin transcriptional activity. J Biol Chem 282: 11221-11229, 2007.
35. Mulholland DJ, Dedhar S, Coetzee GA and Nelson CC: Interaction of nuclear receptors with the Wnt/beta-catenin/Tcf signaling axis: Wnt you like to know? Endocr Rev 26: 898-915, 2005.
36. Daugherty RL and Gottardi CJ: Phospho-regulation of Beta-catenin adhesion and signaling functions. Physiology (Bethesda) 22: 303-309, 2007.
37. Han J, Xie C, Pei T, Wang J, Lan Y, Huang K, Cui Y, Wang F, Zhang J, Pan S, *et al*: Deregulated AJAP1/β-catenin/ZEB1 signaling promotes hepatocellular carcinoma carcinogenesis and metastasis. Cell Death Dis 8: e2736, 2017.

38. Higuchi T, Yokobori T, Naito T, Kakinuma C, Hagiwara S, Nishiyama M and Asao T: Investigation into metastatic processes and the therapeutic effects of gemcitabine on human pancreatic cancer using an orthotopic SUIT-2 pancreatic cancer mouse model. Oncol Lett 15: 3091-3099, 2018.
39. Lu Z, Ghosh S, Wang Z and Hunter T: Downregulation of caveolin-1 function by EGF leads to the loss of E-cadherin, increased transcriptional activity of beta-catenin, and enhanced tumor cell invasion. Cancer Cell 4: 499-515, 2003.
40. Jing Y, Cui D, Guo W, Jiang J, Jiang B, Lu Y, Zhao W, Wang X, Jiang Q, Han B and Xia S: Activated androgen receptor promotes bladder cancer metastasis via Slug mediated epithelial-mesenchymal transition. Cancer Lett 348: 135-145, 2014.
41. Gunthert U, Hofmann M, Rudy W, Reber S, Zöller M, Haussmann I, Matzku S, Wenzel A, Ponta H and Herrlich P: A new variant of glycoprotein CD44 confers metastatic potential to rat carcinoma cells. Cell 65: 12-24, 1991.
42. Nagano O and Saya H: Mechanism and biological significance of CD44 cleavage. Cancer Sci 95: 930-935, 2004.
43. Ponta H, Sherman L and Herrlich PA: CD44: From adhesion molecules to signalling receptors. Nat Rev Mol Cell Biol 4: 33-45, 2003.
44. van Grevenstein WM, Hofland LJ, Jeekel J and van Eijck CH: The expression of adhesion molecules and the influence of inflammatory cytokines on the adhesion of human pancreatic carcinoma cells to mesothelial monolayers. Pancreas 32: 396-402, 2006.
45. Abugomaa A, Elbadawy M, Yamawaki H, Usui T and Sakaki K: Emerging roles of cancer stem cells in bladder cancer progression, tumorigenesis, and resistance to chemotherapy: A potential therapeutic target for bladder cancer. Cells 9: 235, 2020.
46. Brunner A, Prelog M, Verdorfer I, Tzankov A, Mikuz G and Ensinger C: EpCAM is predominantly expressed in high grade and advanced stage urothelial carcinoma of the bladder. J Clin Pathol 61: 307-310, 2008.
47. Xia P and Xu X: PI3K/Akt/mTOR signaling pathway in cancer stem cells: From basic research to clinical application. Am J Cancer 5: 1602-1609, 2015.
48. Matsubara S, Ding Q, Miyazaki Y, Kuwahara T, Tsukasa K and Takao S: mTOR plays critical roles in pancreatic cancer stem cells through specific and stemness-related functions. Sci Rep 3: 3230, 2013.
49. Deshmukh A, Deshpande K, Arfuso F, Newsholme P and Dharmarajan A: Cancer stem cell metabolism: A potential target for cancer therapy. Mol Cancer 15: 69, 2016.
50. Cao ZQ, Wang Z and Leng P: Aberrant N-cadherin expression in cancer. Biomed Phamacother 118: 109320, 2019.
51. Magaway C, Kim E and Jacinto E: Targeting mTOR and metabolism in cancer: Lessons and innovations. Cells 8: 1584, 2019.
52. Valvezan AJ and Manning BD: Molecular logic of mTORC1 signalling as a metabolic rheostat. Nat Metab 1: 321-333, 2019.
53. Zou Z, Tao T, Li H and Zhu X: mTOR signaling pathway and mTOR inhibitors in cancer: Progress and challenges. Cell Biosci 10: 31, 2020.
54. Prossomariti A, Piazzi G, Alquati C and Ricciardiello L: Are Wnt/β-catenin and PI3K/AKT/MTORC1 distinct pathways in colorectal cancer. Cell Mol Gastroenterol Hepatol 10: 491-506, 2020.
55. Liu Y, Lin F, Chen Y, Wang R, Liu J, Jin J and An R: Cryptotanshinone inhibits bladder cancer cell proliferation and promotes apoptosis via the PTEN/PI3K/AKT pathway. J Cancer 11: 488-499, 2020.